PAPER

Spectroscopic characterization of van der Waals interactions in a metal organic framework with unsaturated metal centers: MOF-74–Mg

IOP PUBLISHING JOURNAL OF PHYSICS: CONDENSED MATTER
J. Phys.: Condens. Matter **24** (2012) 424203 (8pp) doi:10.1088/0953-8984/24/42/424203

Spectroscopic characterization of van der Waals interactions in a metal organic framework with unsaturated metal centers: MOF-74–Mg

Nour Nijem[1], Pieremanuele Canepa[2], Lingzhu Kong[3], Haohan Wu[4], Jing Li[4], Timo Thonhauser[2] and Yves J Chabal[1]

[1] Department of Materials Science and Engineering, University of Texas at Dallas, TX 75080, USA
[2] Department of Physics, Wake Forest University, Winston-Salem, NC 27109, USA
[3] Department of Physics and Astronomy, Rutgers University, Piscataway, NJ 08554, USA
[4] Department of Chemistry and Chemical Biology, Rutgers University, Piscataway, NJ 08854, USA

E-mail: Chabal@utdallas.edu

Received 2 April 2012, in final form 26 June 2012
Published 3 October 2012
Online at stacks.iop.org/JPhysCM/24/424203

Abstract
The adsorption energies of small molecules in nanoporous materials are often determined by isotherm measurements. The nature of the interaction and the response of the host material, however, can best be studied by spectroscopic methods. We show here that infrared absorption and Raman spectroscopy measurements together with density functional theory calculations, utilizing the novel van der Waals density functional vdW-DF, constitute a powerful approach to studying the weak van der Waals interactions associated with the incorporation of small molecules in these materials. In particular, we show how vdW-DF assists the interpretation of the vibrational spectroscopy data to uncover the binding sites and energies of these molecules, including the subtle dependence on loading of the IR asymmetric stretch mode of CO_2 when adsorbed in MOF-74–Mg. To gain a better understanding of the adsorption mechanism of CO_2 in MOF-74–Mg, the results are compared with CO within MOF-74–Mg.

(Some figures may appear in colour only in the online journal)

1. Introduction

Physisorption—as a method to facilitate hydrogen storage and CO_2 capture—has attracted much attention, as it is less expensive than conventional methods often using aqueous ammonia and amine functionalized solids [1, 2]. A promising class of materials for such applications includes metal organic frameworks (MOFs) [3–5]. MOFs are porous coordination polymers that are comprised of organic linkers and metal centers (or clusters). Room temperature synthesis, solvothermal heating, microwave assisted heating and electrical heating are some of the methods that have been employed for the design of these materials [6]. The differences in the synthetic methods often lead to different products, even if the starting material is the same. Some MOFs' properties such as their high surface areas, crystallinity, porosity and structural tailorability, have made them attractive for a variety of applications beyond that of gas separation and storage [3]. Potential applications of MOFs have been in catalysis, sensing and biomedical applications [7–10].

Gas adsorption isotherms have typically been used to derive information about the uptake and binding energy of gases in these nanoporous materials. However, these measurements cannot provide microscopic information about the nature of the interaction between the gas guest and the porous host. Details on such interactions are more readily accessible through vibrational spectroscopy (IR absorption and Raman scattering), with the critical input of density functional theory calculations (using the van der Waals density functional vdW-DF developed by Langreth and

co-workers). This combination has provided much insight into gas interactions in the pores of these materials [11–17]. In this paper, the spectroscopic and theoretical approaches are first described using recent studies on hydrogen and CO_2 interactions in MOFs. Then, the specific case of CO_2 and CO adsorption in a well-studied MOF with unsaturated metal centers is investigated, focusing on both CO_2 and CO in MOF-74–Mg, as a function of loading. The information about the specific gas/MOF interaction is mostly derived from IR spectroscopy and vdW-DF calculations. The interaction of CO_2 with MOF-74–Mg is also compared to that of CO, the adsorption of which is largely triggered by its dipole moment. The absorption of CO with MgO surfaces [18–20] and more recently in MOF-74–Mg [21] has been previously studied experimentally and will therefore only be considered from a theoretical stand point to better understand the remarkably different interactions of these two molecules with MOF-74–Mg. While CO_2 only interacts with non-local vdW forces with the Mg^{2+} sites, CO interacts electrostatically accompanied by well-established back-electron transfer phenomena particular to the latter molecule [22, 23].

1.1. Methods probing van der Waals interactions and properties of small molecules in MOFs

Van der Waals interactions involve weak attractive forces that dominate when molecules are at a distance from each other or, in the case of nanoporous materials, at a distance from the walls; the interaction in this case is dictated by dispersive forces. To study such interactions at the atomistic level, we combine spectroscopic techniques such as infrared (IR) and Raman spectroscopy, with computational *ab initio* methods.

1.1.1. IR absorption spectroscopy and Raman scattering. Different methods for IR characterization of gas adsorption exist and depend on the configuration and the type of sample studied. The powder sample can be pressed on a KBr substrate so as to be measured in transmission, or deposited in a crucible and measured using a diffuse reflectance infrared Fourier transform (DRIFT) [24]. For transmission, the total amount of powder used is determined mostly by its absorption and scattering of IR radiation. On the other hand, the DRIFT method offers an easier and faster alternative in terms of sample preparation and amount of sample that can be studied. In DRIFT, the IR beam undergoes multiple refraction, diffraction and absorption events in the sample before reemerging, which increases the IR path length.

Raman scattering is a complementary technique to IR absorption spectroscopy. The physical principles of both are different: infrared radiation is absorbed due to transitions between two vibrational levels of the molecule in its electronic ground state [25]; in contrast, Raman spectra originate from electronic absorption as a response to ultraviolet, visible and near IR radiation, and therefore probes changes in polarization of the molecules.

Interactions of molecules such as H_2, CO_2, H_2O and CH_4 can be investigated using both IR spectroscopy and Raman scattering because a subset of their normal modes are IR or Raman active. The interaction with the substrate affects the frequency and IR activity of the vibration modes of these molecules. As an example, the free H_2 molecule is not IR active (but it is Raman active) because of the lack of a dipole moment. However, the interaction with the substrate induces a dipole moment, allowing some IR activity. CO_2 is both IR and Raman active, the asymmetric stretch mode is IR active and is observed at 2349 cm^{-1}, the symmetric stretch mode is only Raman active and is observed at 1388 cm^{-1}.

CO_2 interaction with different chemical environment usually causes a shift in its asymmetric and symmetric stretch modes. As an example, the interaction of CO_2 through its oxygen end causes a notable shift of its asymmetric stretch mode, a ~ -8 cm^{-1} red-shift for instance for CO_2 in Ni_2(dhtp) [dhtp = 2,5-dihydroxyterphthalate] (also known as MOF-74–Ni with an unsaturated metal center) [26]. Similarly, Vimont *et al* have shown that IR spectroscopy is useful for studying water interactions in the MOF MIL(100) [27]. Raman spectroscopy is particularly useful to detect small structural changes caused by gas adsorption because the framework vibrational modes are sharp and sensitive to the structure, as was observed for CO_2 adsorption in a flexible framework [12].

1.1.2. van der Waals interactions in DFT. DFT in connection with standard functionals is largely ineffective in the description of sparse and soft matter, where van der Waals forces are more likely to dominate. Several strategies have been proposed to include these interactions within DFT [28]. Here, we review some aspects at the foundation of vdW-DF [29], which is a truly non-local functional, capable of capturing non-local effects responsible for vdW forces. The van der Waals interaction of non-polar molecules such as H_2, N_2, CO_2 and CH_4 with MOFs is an excellent application for vdW-DF and some results will be shown below. DFT replaces the complicated system of interacting electrons by a non-interacting electron gas. The missing many-body interaction is incorporated in the exchange–correlation functional, the analytical form of which remains unknown and for practical purposes is approximated. Although the local density (LDA) [30–32] and the generalized gradient approximation (GGA) [33–36] have allowed us to address important issues, they yield qualitatively erroneous results when applied to long-range interactions [28]. In this respect, previous theoretical investigations [13, 15] of H_2 adsorption in MOFs have pointed out the erratic behavior of common LDA and GGA functionals when trying to reproduce experimental quantities such as adsorption energies and other properties. vdW-DF [29] includes an explicit non-local term necessary for the description of non-local van der Waals interactions. Here, the exchange part is taken from revPBE (GGA) [29]. The correlation contribution consists of two parts: (i) the local short-range contribution simply approximated by LDA and (ii) the long-range effects that depend on the electron charge density in a non-local way. The non-local correlation part does not include any empirical or fitted parameters, resulting in high transferability

of this functional. More recently, a self-consistent version of vdW-DF [37] and its potential has been proposed. Knowledge of the potential allows us to combine fully self-consistent calculations with routinely structural relaxations. Using an FFT approach to evaluate vdW-DF [38], the computational effort for a simulation of a large system is comparable to that of GGA calculations, making vdW-DF a very attractive and practical computational tool. More specifically, all the theoretical results presented here are obtained using the vdW-DF functional as currently implemented in *PWscf*, which is part of the Quantum-Espresso Package [39].

1.2. Induced dipole and absorption of H_2

Hydrogen adsorption into several different MOFs has been recently studied by Nijem *et al* [13]. These studies show that the IR shifts of adsorbed H_2 do not necessarily correlate with their binding energies. Instead, the red-shifts observed in the IR vibrational stretch modes are a result of the chemical environment at the adsorption site and depend on the type of linkers used (aromatic versus aliphatic). Slightly larger IR shifts are observed for MOFs with aromatic linkers—for example comparing the frequency shift of H_2 observed for Ni(bdc)(ted)$_{0.5}$ with Ni(bodc)(ted)$_{0.5}$, where bdc = 1,4-benzenedicarboxylate, ted = triethylene-diamine and bodc = bicyclo [2.2.2]octane-1,4-dicarboxylate [13, 40]. There is also no observed dependence of the vibrational frequency on the metal center in MOFs with saturated metal centers. Indeed, vdW-DF calculations not only confirm these observations but also show that the alignment of the H_2 molecule parallel to the metal H_2 axis considerably weakens the metal influence on the H_2 internal mode vibration. In the following we show that the combination of IR spectroscopy and vdW-DF calculations is essential to understand the nature of the weak van der Waals interactions. For instance, the binding energy of H_2 in Zn(bdc)(ted)$_{0.5}$ was calculated to be 5–5.3 kJ mol^{-1} [41] and 6.5–8.3 kJ mol^{-1} for $Ni_3(COOH)_6$ [42]. On the other hand, the IR shifts of H_2 were found to be 8 cm^{-1} larger for the former than the latter. These results indicate that the binding energies and the IR shifts are not necessarily always correlated. Within the MOF unit cell, the potential well may be deep with a high diffusion barrier, yet with a shallow curvature that hardly perturbs the H_2 internal mode.

Another important aspect that came out of the study is that the intensity of the H_2 internal mode cannot be easily used to deduce H_2 concentration because the H_2 stretch dipole moment is strongly affected by the adsorption geometry of the site and H_2–H_2 interactions. As an example, the IR intensity of the H_2 adsorbed in Zn_2(bpdc)$_2$(bpee) [43, 44], where bpdc = 4,4′-biphenyl dicarboxylate and bpee is 1,2-bis(4-pyridyl) ethylene, shows an enhancement factor of 10 as compared to the Zn(bdc)(ted)$_{0.5}$ system, where bdc = 1,4-benzenedicarboxylate and ted = triethylenediamine, although the adsorption isotherms show a 30% larger uptake for Zn(bdc)(ted)$_{0.5}$ as compared to Zn_2(bpdc)$_2$(bpee).

VdW-DF calculations have brought insight by determining, for instance, that the adsorption sites positions for H_2 in both Zn_2(bpdc)$_2$(bpee) and Zn(bdc)(ted)$_{0.5}$ were different [13, 15]. The IR intensity enhancement was shown to be a result of the asymmetry of the adsorption sites and the larger interaction of H_2 with several benzene rings. This surprising observation indicates that the dipole moment and therefore the IR intensity cannot be a measure of the amount adsorbed since it depends on several other factors.

The effect of H_2–H_2 interactions on the IR shifts and dipole moment strength was also studied in MOF-74. The results clearly show that the IR shifts and the dipole moments are affected by these interactions [11, 14]. A study of the IR frequency and dipole moment of H_2 at the primary unsaturated metal site as a function of loading revealed frequency shifts and dipole moment variations specifically induced by the occupation of H_2 at neighboring sites and near neighboring sites. For example, the IR intensity of the IR vibration mode corresponding to the H_2 adsorbed at the metal site in MOF-74–Co was shown to decrease in intensity as the H_2 occupies the low binding energy 'benzene' site [11]. These studies show that the dipole moment of H_2 adsorbed at a high binding energy site, such as the metal site in MOF-74, is affected by H_2 adsorbed at a neighboring site. Moreover, it also points to the influence of lower binding energy sites such as the benzene sites in MOF-74 for H_2 storage.

1.3. Molecules with strong IR absorption

Molecules such as CO_2 with a strong IR absorption mode due to the asymmetric stretch are sensitive to the adsorption environment and the specific interactions with the walls of the framework. While CO_2 has no static dipole moment, it has a large quadrupole moment and a high polarizability (29.11×10^{18}/esu cm). This large quadrupole moment affects the way that it interacts with acidic or basic sites, which makes CO_2 a sensitive probe of the nature of bonding sites.

As an example, Cu-TDPAT is an *rht*-type MOF built from supramolecular building blocks using 2,4,6-tris(3,5-dicarboxylphenylamino)-1,3,5-triazine (H_6TDPAT) linkers. Cu-TDPAT has a high density of open metal sites (OMS) and Lewis-basic sites (LBSs) with high surface area (1938 m^2 g^{-1}) and pore volume (0.93 cm^3 g^{-1}) [45]. Therefore, we would expect CO_2 to have its internal modes accordingly affected by the binding geometry. Indeed three IR absorption bands are observed as a result of the presence of different adsorption environments [45].

An interesting property of some MOFs is the possibility of reversible structural changes as a response to external stimuli such as gas adsorption, making them more attractive than zeolites and carbon materials for specialized applications [46]. This property makes their structures more functional as discussed in a review paper by Kitagawa *et al* [47].

Flexible frameworks often exhibit selectivity, which makes them interesting for gas separation application. The interaction between the adsorbate and the surface of the framework in some MOFs causes an expansion of the pore size, referred to as gate opening. This phenomenon is often identified by a step in the isotherm and a hysteresis in the adsorption desorption measurements [47–55]. In many

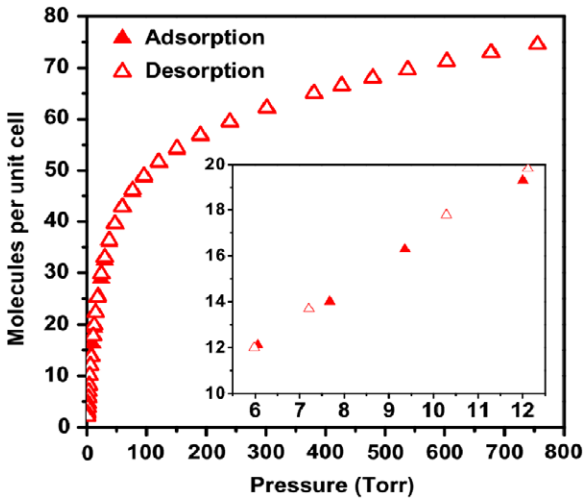

Figure 1. Adsorption (closed symbol) and desorption (open symbols) isotherms of CO_2 at room temperature in MOF-74–Mg.

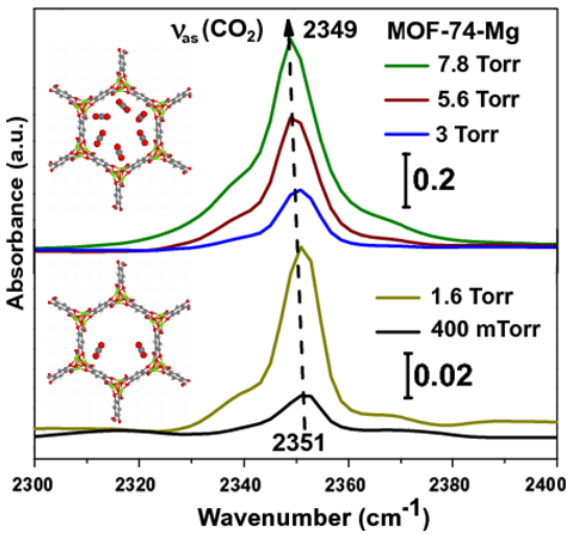

Figure 2. IR absorption spectra of CO_2 in MOF-74–Mg as a function of pressure at 298 K. The inset shows a scheme for the case for low loading and full loading calculated using vdW-DF.

cases, a combination of x-ray diffraction and isotherm studies gives the necessary information about the understanding of geometrical transformation.

IR absorption and Raman scattering have brought insight into effects causing framework flexibility, such as effects caused by changes in the chemical environment. An example is the recent spectroscopic study performed on MIL-47(V^{IV}), MIL-47(V^{III}). The study explored the influence of the oxidation state of the metal center on the MOF flexibility [56].

Moreover, some of the MOFs lack a hysteresis in the adsorption isotherm, due to a fast response of the framework to the pressure change. An example is the stepped isotherm with no hysteresis in the CO_2 adsorption isotherm of $Zn_2(bpdc)_2(bpee)$ [57]. An explanation for the stepped isotherm in some of the MOFs was attributed to CO_2–CO_2 interactions as suggested by Walton *et al* [58]. A convenient way to check for structural changes is the use of Raman spectroscopy.

Raman spectroscopy is a relatively common spectroscopic technique as compared to *in situ* x-ray diffraction and has brought much insight into the adsorption and interaction of small molecules in MOFs [12, 27, 59–61]. For instance, flexible structural changes have been monitored by Raman spectroscopy as was shown in studies of MIL-53 (Ga, Cr) [62].

The study performed on $Zn_2(bpdc)_2(bpee)$ illustrated the role of Raman spectroscopy in understanding the origin of the stepped isotherm.

A combination of Raman spectroscopy and vdW-DF calculations uniquely showed that there are structural changes occurring in $Zn_2(bpdc)_2(bpee)$, even though there is no hysteresis observed in the isotherm. The MOFs flexibility was attributed to: (1) the monodentate carboxylate connectivity at the metal node and (2) the presence of a flexible linker responding only to molecules with high quadrupole moment, such as a bpdc linker, and responsible for high CO_2 selectivity, providing a guide for tailored synthesis [12].

2. IR study of CO_2 loading in MOF-74–Mg

To test whether the IR frequency shift of CO_2 can also be affected by the loading of CO_2 and the occupation of other sites, we have performed IR absorption spectroscopy measurements and vdW-DF calculations on MOF-74–Mg. The IR measurements are performed in transmission at room temperature as a function of CO_2 pressure in the region 700 mTorr–8 Torr for MOF-74–Mg as shown in figure 2. The isotherm measurements are performed for CO_2 adsorption in MOF-74–Mg, revealing that a pressure of ∼12 Torr is needed for occupation of all the metal sites as shown in figure 1. The IR measurements show that at low pressures there is a ∼3 cm^{-1} blue-shift in the asymmetric stretch mode of adsorbed CO_2 as compared to the unperturbed asymmetric stretch mode of CO_2 at 2349 cm^{-1}. This shift is consistent with an interaction of the CO_2 through its oxygen with the unsaturated metal center [63]. As the pressure is increased to ∼6 Torr, a pressure at which the isotherms show occupation of 12 CO_2/unit cell (the unit cell has 18 Mg metal centers), the IR frequency shift is lowered to a value similar to the gas-phase asymmetric stretch mode at 2349 cm^{-1}.

This red-shift can be explained as an effect of CO_2–CO_2 interactions between neighboring sites as more metal sites are occupied. Such an effect will cause a change of the CO_2 interaction with the metal center from its initially adsorbed position, and therefore will cause a CO_2 frequency change. Indeed, vdW-DF calculations described below show that there are changes from the isolated case in the CO_2 interaction with the metal center.

Infrared spectroscopy is best to study the effect of loading. However, the very high IR absorption of the CO_2 gas phase as the pressure is increased above 10 Torr leads to saturation of the signal. Therefore, to study loadings beyond the occupation of the six metal sites per primitive unit cell, a different experimental procedure was employed. The sample

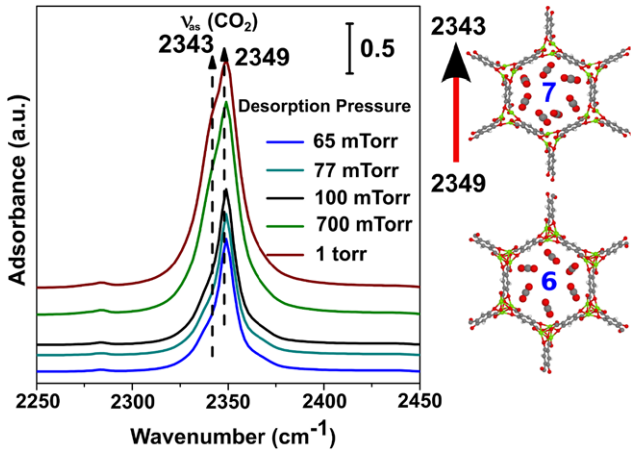

Figure 3. IR absorption of CO_2 adsorbed in MOF-74–Mg as a function of desorption pressure after exposure to 1 kTorr (1 atm) of CO_2.

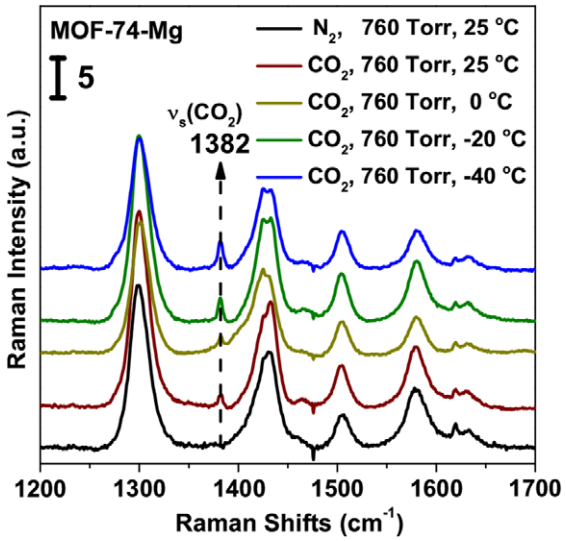

Figure 4. Raman spectra of MOF-74–Mg under 1 atm of N_2 and CO_2 as a function of temperature.

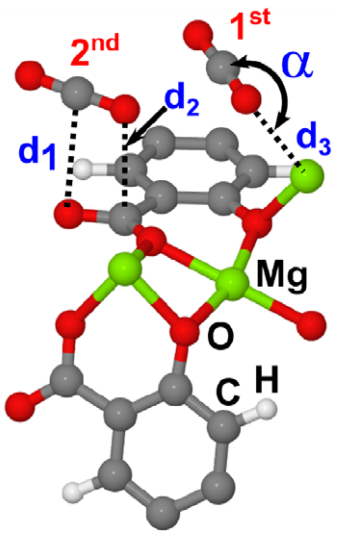

Figure 5. Local view of the primary (1st) and secondary (2nd) sites where CO_2 molecules bind in the MOF-74–Mg structure, along with relevant bond lengths and angles.

was first exposed to 1 kTorr (1 atm) of CO_2 gas and then the chamber was evacuated. The IR spectra were recorded as a function of desorption pressure and are summarized in figure 3. This procedure ensures that higher loadings are achieved. The system can then be probed if the kinetics of CO_2 removal are slow enough, as shown in figures 2 and 3, in which the intensities of the main CO_2 IR mode (i.e. amount of CO_2) confirm that a high loading is still present. A main IR band at 2349 cm^{-1} is observed, and is attributed to the asymmetric stretch of CO_2 when most of the metal sites are occupied. It can be noted that at the highest desorption pressure ∼1 Torr a shoulder at 2343 cm^{-1} is observed. This shoulder decreases in intensity as the pressure is reduced. This additional IR band can be attributed to the CO_2 adsorbed on a secondary site involving one oxygen and one carbon of the organic linker close to two Mg sites (see figure 5). The absence of this mode under the first experimental conditions (figure 2) supports the assignment that this mode is associated with CO_2 at the secondary site after the occupation of all the metal sites. This result is consistent with a recent neutron powder diffraction study by Queen *et al* [64] that clearly identified a similar secondary site.

Raman spectroscopy measurements studying this system were also performed and the results are summarized in figure 4. Figure 4 shows the Raman spectrum of MOF-74–Mg under N_2 atmosphere (1 atm, RT, black spectrum) and under 760 Torr of CO_2 as a function of temperature. The weak Raman mode observed at 1382 cm^{-1} is assigned to the symmetric CO_2 stretch mode ~ -6 cm^{-1} red shifted with respect to the unperturbed CO_2 mode at 1388 cm^{-1}. The red-shift indicates that the interaction with the metal center weakens the CO_2 bond and this is supported by our simulations for the symmetric stretching of CO_2 (see below). While the ΔE measured for higher loadings differ from that of the mono-adsorbed molecule, the theoretical frequency for this mode remains subjected to an additional red-shift (see below). The low intensity of this mode is due to the small Raman cross section of CO_2. The isotherm measurements show that under these conditions ∼70 molecules occupy a unit cell, which indicates that this Raman shift corresponds to the highest loading.

We simulated the loading of CO_2 (and CO) molecules in MOF-74–Mg using vdW-DF. Ultrasoft pseudopotentials with a plane-wave cutoff of 35 Ryd were used to describe the wavefunctions in both MOF-74–Mg and CO_2 (or CO) while the density cutoff was set to 280 Ryd. The convergence threshold for the total energy was set to 5×10^{-12} Ryd, ensuring an accurate sampling of the complex potential energy surface for MOF-74–Mg. The MOF-74 structure with CO_2 (or CO) was relaxed using vdW-DF until the force criterion, i.e. 1×10^{-5} Ryd/bohr, was satisfied. The hexagonal lattice parameters of MOF-74–Mg were fixed according to the experimental values, i.e. $a = 25.887$ Å and $c = 6.816$ Å [65]. The IR frequencies for CO_2 (and CO) were calculated

Table 1. Adsorption energies, ΔE, (in kJ mol^{-1}) of CO and CO_2 in MOF-74–Mg at different loadings. M is CO or CO_2, α (deg) is the angle formed between the molecule and the Mg site in the MOF structure, whereas θ (%) is the saturation of Mg^{2+} centers in the MOF.

		ΔE		α	
No. M	θ	CO	CO_2	CO	CO_2
1	16.7	−31.7	−48.2	178.42	126.36
2	33.4	−32.5	−47.0	171.75	147.77
3	50.0	−32.8	−47.0	165.65	142.15
4	67.0	−33.1	−49.2	164.96	141.76
5	83.4	−33.3	−48.0	164.34	138.59
6	100.0	−33.6	−48.3	161.36	138.30

with the same criteria adopted for the ΔE calculations, but increasing the density cutoff to 420 Ryd. The dynamical matrix, at the Γ point, was calculated only for the molecular fragment (i.e. CO_2 or CO) using a five-point formula with a displacement of 0.02 Å. The frequency values for the high-loading situations, six CO_2 or six CO in MOF-74–Mg, were averaged.

There are many possible configurations in which CO_2 can be adsorbed in the MOF structure. Previous studies have largely concluded that non-polar molecules such as H_2, N_2 and CO_2 prefer to interact with the metal sites, i.e. Mg^{2+} in MOF-74–Mg [63]. This effect becomes more pronounced when the metal centers are not fully coordinated. MOF-74 has in total six metal centers in the primitive unit cell that are progressively occupied with CO_2 (or CO) molecules until full saturation is reached. Thus, knowledge of the interactions of CO and the MOF is of crucial importance to understand the difference in adsorption between a polar and a non-polar molecule in such systems. In contrast to the adsorption of CO_2, mostly driven by van der Waals forces, the adsorption of CO is mainly dominated by its dipole moment, and thus helps understand the CO_2 adsorption mechanisms involved. The energy involved in the absorption of CO_2 or CO molecules in the MOF-74–Mg structure, ΔE, is defined as

$$\Delta E = E_{\mathrm{MOF+M}} - (E_{\mathrm{MOF}} + nE_{\mathrm{M}}). \quad (1)$$

Here, $E_{\mathrm{MOF+M}}$, E_{MOF} and E_{M} are the energies of the optimized structures of the MOF + M adduct, MOF alone, and M alone. In our case M is CO or CO_2 and n counts the number of M species introduced. In table 1, we report ΔE for CO and CO_2 at different loadings in MOF-74–Mg.

Both CO and CO_2 adsorb favorably in the MOF-74–Mg structure. The calculated binding energy at the 1 CO_2/primitive unit cell is found to be close to previous values derived from experimental isotherms [64, 66]. Although CO shows a non-vanishing dipole moment, it appears less reactive than CO_2. ΔE decreases as the number of the adsorbed CO molecules increases until complete saturation of the six Mg^{2+} centers. The latter effect remains less obvious for CO_2, where the lateral CO_2–CO_2 interactions play a dominant role (increasing the ΔE values). Repulsive effects are accompanied by the concomitant reduction of the space available for new incoming molecules. This would impose some physical limit to the total number of molecules adsorbed. The angle α formed between the molecule (CO_2 or CO) and the metal site (see [64]) provides insightful information to the distortion of the original adsorption geometry as the molecular loading increases (see table 1). For CO_2, α increases initially (case with two CO_2 molecules per cell) but progressively decreases for situations of high CO_2 loading (three to six molecules per cell). An increase in the magnitude of α is observed for situations of low loading, where more space in the proximity of the adsorption site remains available, offering more steric degrees of freedom for the adsorbed molecule. The contrary occurs in high-loading cases where the interaction of CO_2 with the metal site is subjected to a larger distortion when compared to the mono-adsorbed situation (see table 1), explaining the slight change observed in the experimental CO_2 frequency in figure 2 as the secondary site is occupied. Because CO is smaller than CO_2, the steric effect is not the driving force and the magnitude of α is entirely controlled by repulsive CO–CO interactions. Although CO was initially adsorbed with its C pointing on the metal centers, we also considered an interaction of the CO through its oxygen, Mg–O=C, for which we only report the binding energies for the mono- (−30.4 kJ mol^{-1}) and fully- (−31.3 kJ mol^{-1}) occupied cases, one and six molecules, respectively. The binding energies indicate that an interaction through the oxygen is less energetically favorable than that through the molecule's carbon.

Furthermore, small oscillations in ΔE measured in the CO_2 cases must be linked to the computational strategy adopted; the cell is frozen to the experimental structure. As the Mg^{2+} sites are progressively occupied by new CO_2 molecules, their lateral interactions are not strong enough to introduce substantial changes to their internal molecular structures. ΔE increases to −48.0 kJ mol^{-1} when adsorbing the seventh CO_2 molecule on the secondary site (see figure 5), because the lateral CO_2–CO_2 interactions dominate. Having occupied all six metal sites, new incoming CO_2 molecules are forced to adsorb on the secondary site (see figure 5), which is not preferred for low loading (number of $CO_2 < 6$).

The adsorption geometry of CO_2 in the secondary site has already been determined experimentally by Queen *et al* [64] using neutron powder diffraction, resulting in $d_1 = 3.11$ Å and $d_2 = 3.07$ Å (see figure 5). This experimental geometry is well reproduced by our vdW-DF results of $d_1 = 3.25$ and $d_2 = 3.14$ Å, respectively, confirming the validity of our model. Eventually, the experimental distance of CO_2 from the primary adsorption site, $d_3 = 3.54$ Å, (see figure 5) is slightly overestimated as $d_3 = 4.00$ Å. Furthermore, the corresponding ΔE of −46 kJ mol^{-1}, calculated after relaxing

the ionic positions of the experimental structure of CO_2 in MOF-74–Mg ($a = 25.824$, $c = 6.8904$ Å, see Queen *et al* [64]), is also comparable with results in table 1, although it is slightly larger than that for the adsorption of the seventh CO_2 described above, i.e. -48 kJ mol^{-1}. Our computational investigation in accordance with [64] suggests that the second binding site is only occupied at high loading. Experimentally, it is observed as a shoulder at 2143 cm^{-1} only at higher loadings (figure 3). When the loading is increased, the environment around the second binding sites is modified helping their occupation by incoming molecules. On the other hand, if a CO_2 is initially adsorbed on the second binding site when not all six first binding sites are occupied, then the geometry relaxation leads the molecule to move from the second binding site to the first one. The ΔE values of table 1 are in close agreement with B3LYP + D data, where van der Waals forces are introduced by means of an empirical correction [21, 67].

Our frequency analysis is limited only to the stretching modes of CO_2, ν_3 (asymmetric), ν_1 (symmetric) and ν for CO. The calculated frequencies for ν_3 and ν modes of the gas-phase molecules are at 2340 and 2135 cm^{-1}, respectively. These values are in good agreement with the experimental values for CO_2 observed at 2349 cm^{-1} in this study and for CO at 2143 cm^{-1} observed by Valenzano *et al* [21], enforcing the effectiveness of vdW-DF in reproducing the experimental data.

When one CO_2 is adsorbed in MOF-74–Mg, ν_3 undergoes a blue-shift ($\Delta\nu = 21$ cm^{-1}) to 2363 cm^{-1}. Although the magnitude of the calculated blue-shift is large, due to an overestimation of the vdW-DF method, Poloni *et al* [68] recently calculated a similar blue-shift (17 cm^{-1}) using the same functional. A possible cause of this overestimation can originate in the approximative nature of DFT in general, as well as potential anharmonic effects not considered in our calculations. When CO is introduced in MOF-74–Mg, the CO ν mode is found to blue-shift to 2167 cm^{-1} ($\Delta\nu = 32$ cm^{-1}) consistently with earlier IR measurements ($\Delta\nu = 35$ cm^{-1}) [21]. Our calculated values are found to be very close to the experimental ones. In the case of high loading, i.e. adsorption of six molecules of CO_2 or CO in MOF-74–Mg the CO_2 ν_3 mode is now at 2362 cm^{-1} and suffers a slight additional red-shift ($\Delta\nu = -1$ cm^{-1}) from the mono-adsorbed frequency, while the ν (in CO) mode further blue-shifts to 2170 cm^{-1} ($\Delta\nu = 35$ cm^{-1}, from the mono-adsorbed frequency $\Delta\nu = 3$ cm^{-1}).

Regarding the computed symmetric stretching, the mode ν_1 of CO_2 (at 1390 cm^{-1} as calculated for gas phase CO_2) is found to red-shift to 1375 cm^{-1} ($\Delta\nu = -15$ cm^{-1}) for the mono-adsorbed case. When the loading is further increased to six CO_2 molecules per primitive cell (full loading situation), the mode red-shifts further to 1373 cm^{-1}, with a total $\Delta\nu$ of -17 cm^{-1} from its gas-phase value. Although the gas-phase frequency ν_1 is in nice agreement with the experimental value (1388 cm^{-1}), the computed red-shift remains overestimated when the CO_2 is adsorbed in the MOF. Similar overestimation of the frequency shift was reported by Poloni *et al* using the vdW-DF method [68]. Our calculated red-shift for the seventh CO_2/unit cell might not correlate with the -1 cm^{-1} red-shift observed experimentally, and may also be caused by the dissimilarity in adsorption geometries for each CO_2 in the MOF structure. An alternative source for the small red-shift observed in the computed frequency for the high-loading situations can be due to dissimilarities in the adsorption geometries of each CO_2 in the MOF structure.

The experimental red-shift observed when the loading of CO_2 is increased is confirmed by our experiments (see figure 2), whereas the calculated values for CO at high loadings are found in agreement with the experimental frequency reported in [21].

Although the effect of temperature is not considered in these simulations, on the basis of our binding energies we expect that CO_2 can selectively replace CO though dynamical effects once adsorbed in the MOF-74–Mg structure.

3. Summary and outlook

IR and Raman absorption spectroscopy in combination with vdW-DF calculations are crucial in the understanding of van der Waals interactions in porous materials. Previous studies show that the CO_2 IR stretch mode is sensitive to the chemical environment of the adsorption [12, 45]. We also find it to be dependent on the loading (i.e. the occupation of other sites) when the interaction among CO_2 molecules plays a role. CO_2 adsorption in MOF-74–Mg as a function of loading was studied using IR absorption spectroscopy and vdW-DF calculations. A slight red-shift ($\Delta\nu = -2$ cm^{-1}) of the IR frequency of the adsorbed CO_2 stretch mode from the isolated case, is observed both experimentally and theoretically as a result of CO_2–CO_2 interactions at high loadings (6 CO_2/primitive unit cell). An additional secondary adsorption site was identified by vdW-DF and IR absorption spectroscopy.

Future work in understanding the diffusion of molecules such as CO_2, H_2 and other molecules into MOFs is of interest for many practical applications. The co-adsorption of molecules in MOFs should be addressed both theoretically and experimentally in order to gain a better understanding of its effect on the interaction. This understanding, in turn, will then lead to the design of better framework materials with enhanced properties.

Acknowledgments

This work was supported in its totality by the Department of Energy, Basic Energy Sciences, division of Materials Sciences and Engineering (DOE grant No. DE-FG02-08ER46491).

References

[1] Liu J, Thallapally P K, McGrail B P, Brown D R and Liu J 2012 *Chem. Soc. Rev.* **41** 2308
[2] Murray L J, Dinca M and Long J R 2009 *Chem. Soc. Rev.* **38** 1294
[3] Suh M P, Park H J, Prasad T K and Lim D-W 2012 *Chem. Rev.* **112** 782

[4] Sumida K, Rogow D L, Mason J A, McDonald T M, Bloch E D, Herm Z R, Bae T-H and Long J R 2012 *Chem. Rev.* **112** 724
[5] Li J-R, Sculley J and Zhou H-C 2012 *Chem. Rev.* **112** 869
[6] Stock N and Biswas S 2012 *Chem. Rev.* **112** 933
[7] Keskin S and Seda K 2011 *Indust. Eng. Chem.* **50** 1799
[8] Horcajada P, Gref R, Baati T, Allan P K, Maurin G, Couvreur P, Ferey G, Morris R E and Serre C 2012 *Chem. Rev.* **112** 1232
[9] Kreno L E, Leong K, Farha O K, Allendorf M, van Duyne R P and Hupp J T 2012 *Chem. Rev.* **112** 1105
[10] Yoon M, Srirambalaji R and Kim K 2012 *Chem. Rev.* **112** 1196
[11] Nijem N, Kong L, Zhao Y, Wu H, Li J, Langreth D C and Chabal Y J 2011 *J. Am. Chem. Soc.* **133** 4782
[12] Nijem N *et al* 2011 *J. Am. Chem. Soc.* **133** 12849
[13] Nijem N, Veyan J-F, Kong L, Li K, Pramanik S, Zhao Y, Li J, Langreth D and Chabal Y J 2010 *J. Am. Chem. Soc.* **132** 1654
[14] Nijem N, Veyan J-F O, Kong L, Wu H, Zhao Y, Li J, Langreth D C and Chabal Y J 2010 *J. Am. Chem. Soc.* **132** 14834
[15] Kong L, Cooper V R, Nijem N, Li K, Li J, Chabal Y J and Langreth D C 2009 *Phys. Rev.* B **79** 081407
[16] Langreth D C, Dion M, Rydberg H, Schroder E, Hyldgaard P and Lundqvist B I 2005 *Int. J. Quantum Chem.* **101** 599
[17] Lamberti C, Zecchina A, Groppo E and Bordiga S 2010 *Chem. Soc. Rev.* **39** 4951
[18] Zecchina A, Coluccia S, Spoto G, Scarano D and Marchese L 1990 *J. Chem. Soc. Faraday Trans.* **86** 703
[19] Marchese L, Coluccia S, Martra G, Giamello E and Zecchina A 1991 *Mater. Chem. Phys.* **29** 437
[20] Damin A, Dovesi R, Zecchina A and Ugliengo P 2001 *Surf. Sci.* **479** 255
[21] Valenzano L, Civalleri B, Chavan S, Palomino G T, Arean C O and Bordiga S 2010 *J. Phys. Chem.* C **114** 11185
[22] Pacchioni G, Cogliandro G and Bagus P S 1991 *Surf. Sci.* **255** 344
[23] Zecchina A, Spoto G, Coluccia S and Guglielminotti E 1984 *J. Phys. Chem.* **88** 2575
[24] FitzGerald S A, Churchill H O H, Korngut P M, Simmons C B and Strangas Y E 2006 *Rev. Sci. Instrum.* **77** 093110
[25] Kazuo N 1997 *Infrared and Raman Spectra of Inorganic and Coordination Compounds* 5 edn, vol 1 (New York: Wiley)
[26] Dietzel P D C, Johnsen R E, Fjellvag H, Bordiga S, Groppo E, Chavan S and Blom R 2008 *Chem. Commun.* 5125
[27] Vimont A, Goupil J-M, Lavalley J-C, Daturi M, Surble S, Serre C, Millange F, Ferey G and Audebrand N 2006 *J. Am. Chem. Soc.* **128** 3218
[28] French R H *et al* 2010 *Rev. Mod. Phys.* **82** 1887
[29] Langreth D C *et al* 2009 *J. Phys.: Condens. Matter* **21** 084203
[30] Ceperley D M and Alder B J 1980 *Phys. Rev. Lett.* **45** 566
[31] Perdew J P and Zunger A 1981 *Phys. Rev.* B **23** 5048
[32] Vosko S H, Wilk L and Nusair M 1980 *Can. J. Phys.* **58** 1200
[33] Perdew J P and Yue W 1986 *Phys. Rev.* B **33** 8800
[34] Perdew J P, Burke K and Ernzerhof M 1996 *Phys. Rev. Lett.* **77** 3865
[35] Becke A D 1988 *Phys. Rev.* A **38** 3098
[36] Lee C, Yang W and Parr R G 1988 *Phys. Rev.* B **37** 785
[37] Thonhauser T, Cooper V R, Li S, Puzder A, Hyldgaard P and Langreth D C 2007 *Phys. Rev.* B **76** 125112
[38] Roman-Perez G and Soler J M 2009 *Phys. Rev. Lett.* **103** 096102
[39] Giannozzi P *et al* 2009 *J. Phys.: Condens. Matter* **21** 395502
[40] Li K, Lee J, Olson D H, Emge T J, Bi W, Eibling M J and Li J 2008 *Chem. Commun.* 6123
[41] Lee J Y, Olson D H, Pan L, Emge T J and Li J 2007 *Adv. Funct. Mater.* **17** 1255
[42] Kunhao L, David H O, Jeong Yong L, Wenhua B, Ke W, Tan Y, Qiang X and Li J 2008 *Adv. Funct. Mater.* **18** 2205
[43] Lan A, Li K, Wu H, Olson D H, Emge T J, Ki W, Hong M and Li J 2009 *Angew. Chem. Int. Edn* **48** 2334
[44] Lan A *et al* 2009 *Inorg. Chem.* **48** 7165
[45] Li B *et al* 2012 *Angew. Chem. Int. Edn* **51** 1412
[46] Sareeya B, Satoru S and Susumu K 2008 *Sci. Tech. Adv. Mater.* **9** 014108
[47] Kitagawa S, Kitaura R and Noro S-I 2004 *Angew. Chem. Int. Edn* **43** 2334
[48] Tanaka D, Nakagawa K, Higuchi M, Horike S, Kubota Y, Kobayashi T C, Takata M and Kitagawa S 2008 *Angew. Chem.* **120** 3978
[49] Salles F *et al* 2010 *J. Am. Chem. Soc.* **132** 13782
[50] Kitagawa H 2009 *Nature Chem.* **1** 689
[51] Ferey G and Serre C 2009 *Chem. Soc. Rev.* **38** 1380
[52] Ferey G 2008 *Chem. Soc. Rev.* **37** 191
[53] Demessence A and Long J R 2010 *Chem. Eur. J.* **16** 5902
[54] Bureekaew S, Shimomura S and Kitagawa S 2008 *Sci. Tech. Adv. Mater.* **9** 014108
[55] Culp J T, Smith M R, Bittner E and Bockrath B 2008 *J. Am. Chem. Soc.* **130** 12427
[56] Leclerc H, Devic T, Devautour-Vinot S, Bazin P, Audebrand N, Ferey G, Daturi M, Vimont A and Clet G 2011 *J. Phys. Chem.* C **115** 19828
[57] Wu H, Reali R S, Smith D A, Trachtenberg M C and Li J 2010 *Chem. Eur. J.* **16** 13882
[58] Walton K S, Millward A R, Dubbeldam D, Frost H, Low J J, Yaghi O M and Snurr R Q 2007 *J. Am. Chem. Soc.* **130** 406
[59] Rosman N, Abello L, Chabert J P, Verven G and Lucazeau G 1995 *J. Appl. Phys.* **78** 519
[60] Centrone A, Siberio-Pérez D Y, Millward A R, Yaghi O M, Matzger A J and Zerbi G 2005 *Chem. Phys. Lett.* **411** 516
[61] Siberio-Perez D Y, Wong-Foy A G, Yaghi O M and Matzger A J 2007 *Chem. Mater.* **19** 3681
[62] Hamon L *et al* 2009 *J. Am. Chem. Soc.* **131** 17490
[63] Yao Y, Nijem N, Li J, Chabal Y J, Langreth D C and Thonhauser T 2012 *Phys. Rev.* B **85** 064302
[64] Queen W L, Brown C M, Britt D K, Zajdel P, Hudson M R and Yaghi O M 2011 *J. Phys. Chem.* C **115** 24915
[65] Dietzel P D C, Besikiotis V and Blom R 2009 *J. Mater. Chem.* **19** 7362
[66] Britt D, Furukawa H, Wang B, Glover T G and Yaghi O M 2009 *Proc. Natl Acad. Sci.* **106** 20637
[67] Valenzano L, Civalleri B, Sillar K and Sauer J 2011 *J. Phys. Chem.* C **115** 21777
[68] Poloni R, Smit B and Neaton J B 2012 *J. Phys. Chem.* A **116** 4957